

# Agglomeration of Silver Nanoparticles in Sea Urchin

**Sunthon Piticharoenphun, Lidiya Šiller**

Newcastle University, School of Chemical Engineering and Advanced Materials

Newcastle upon Tyne, NE1 7RU, United Kingdom

[sunthon.piticharoenphun@ncl.ac.uk](mailto:sunthon.piticharoenphun@ncl.ac.uk); [lidiya.siller@ncl.ac.uk](mailto:lidiya.siller@ncl.ac.uk)

**Marie-Louise Lemloh**

Universität Stuttgart, Biologisches Institut-Abteilung Zoologie

Pfaffenwaldring 57, 70569 Stuttgart, Germany

[marie-louise.lemloh@bio.uni-stuttgart.de](mailto:marie-louise.lemloh@bio.uni-stuttgart.de)

**Murielle Salome, Marine Cotte**

European Synchrotron Radiation Facility, X-ray and FTIR Microspectroscopy Beamline ID21

B.P. 220-38043, Grenoble, Cedex, France

[salome@esrf.fr](mailto:salome@esrf.fr); [cotte@esrf.fr](mailto:cotte@esrf.fr)

**Burkhard Kaulich**

Diamond Light Source, Diamond House

Harwell Science and Innovation Campus, Didcot, Oxfordshire, OX11 0DE, United Kingdom

[burkhard.kaulich@diamond.ac.uk](mailto:burkhard.kaulich@diamond.ac.uk)

**Alessandra Gianoncelli**

Elettra-Sincrotrone Trieste, TwinMic Beamline

Strada Statale 14, km 163.5 in Area Science Park, I-34149 Trieste-Basovizza, Italy

[alessandra.gianoncelli@elettra.trieste.it](mailto:alessandra.gianoncelli@elettra.trieste.it)

**Budhika G. Mendis**

Durham University, Department of Physics

South Road, Durham, DH1 3LE, United Kingdom

[b.g.mendis@durham.ac.uk](mailto:b.g.mendis@durham.ac.uk)

**Ursel Bangert**

The University of Manchester, School of Materials

Oxford Road, Manchester, M13 9PL, United Kingdom

[ursel.bangert@manchester.ac.uk](mailto:ursel.bangert@manchester.ac.uk)

**Nigel R. J. Poolton**

European XFEL, Notkestrasse 85, 22607

Hamburg, Germany

[nigel.poolton@xfel.eu](mailto:nigel.poolton@xfel.eu)

## **Benjamin R. Horrocks**

Newcastle University, School of Chemistry  
 Newcastle upon Tyne, NE1 7RU, United Kingdom  
 b.r.horrocks@ncl.ac.uk

## **Franz Brümmer**

Universität Stuttgart, Biologisches Institut-Abteilung Zoologie  
 Pfaffenwaldring 57, 70569 Stuttgart, Germany  
 franz.bruemmer@bio.uni-stuttgart.de

## **Davorin Medaković**

Ruder Boškovic Institute, Center for Marine Research  
 Giordano Paliaga 5, 52210 Rovinj, Croatia  
 davorin.medakovic@irb.hr

**Abstract-** Silver nanoparticles (AgNPs) are one of the most important nanomaterials for toxicological study due to their extensive use in consumer products and their potential effects on both human and animal health, and the environment. There is, however, insufficient information on their impact on the marine environment. Here, we study the effect of AgNPs in sea urchin (*Paracentrotus lividus*) development by X-ray absorption near edge structure (XANES) and Fourier transform infrared (FTIR) spectroscopy. Agglomerated AgNPs were observed in sea urchin larva at 51 h after exposure to AgNPs with a concentration of 0.3 mg/L. XANES shows that agglomerated AgNPs contain oxidized Ag species complexed with S and O/N ligands. FTIR results confirm the presence of additional sulphur compounds suggestive of a biological response to the toxicity of AgNPs in the sea urchins. Additionally, it could be concluded from the FTIR results that there is a loss of calcite in the sea urchins exposed to AgNPs.

**Keywords:** Silver Nanoparticles, Sea Urchins, Toxicity, XANES, XRF, FTIR

© Copyright 2012 Authors - This is an Open Access article published under the Creative Commons Attribution License terms (<http://creativecommons.org/licenses/by/2.0/>). Unrestricted use, distribution, and reproduction in any medium are permitted, provided the original work is properly cited.

dressings and textile fabrics, and they can be added in sanitary processes for antimicrobial purposes (Rai et al., 2009; Drake and Hazelwood, 2005). However, there is growing concern about their toxicity to humans and animals when released into the environment by several routes, such as from synthesis/manufacturing processes and the use of products containing AgNPs (Fabrega et al., 2011).

At present, the mechanism of toxicity from AgNPs is not fully understood. This has stimulated research on the influence of AgNPs on the environment, especially the effect on several kinds of animals such as zebrafish embryos (freshwater organism). The results from these studies show that AgNPs cause mortality of zebrafish embryos when exposed to high concentration of AgNPs, while exposure with low concentrations causes various morphological malformations such as abnormal body axes, twisted notochord, damaged eyes and curved tails, together with developmental delay of the embryos (Bar-Ilan et al., 2009; Asharani et al., 2008; Powers et al., 2010; Yeo and Kang, 2008). In addition, it was found that AgNPs can be distributed in different organs of zebrafish (brain, heart, yolk, blood) (Asharani et al., 2008). AgNP toxicity has also been studied in other aquatic animals, including Japanese medaka (Chae et al., 2009), oyster embryos (Ringwood et al., 2010), rainbow trout (Farkas et al., 2010) and blue mussels (Zuykov et al., 2011).

Sea urchins are one of the more important marine animals in the ecosystem and are often used as model biological system for toxicological studies: they regulate the growth of algal biomass in the sea and also form a source of food for several predators in the aquatic ecosystem. Additionally, sea urchins (such as red sea urchins) are important fishery resources for humans (Pearse, 2006). Sea urchins are one of the most favourable biological systems used in toxicity experiments for a variety of reasons: 1) they spawn a large number of gametes which can be easily

## **1. Introduction**

In recent years there has been extensive use of nanomaterials in various consumer products, including silver nanoparticles (AgNPs); due to their specific and beneficial properties, it is likely that their consumption will continually rise in the future. AgNPs have significant use as an antimicrobial agent, being coated on medical devices, wound

obtained and externally fertilized; 2) their fertilization can be properly manipulated and carried out in the laboratory; 3) the embryo development can be studied within a few days; 4) embryos in the beginning of the development stages are very sensitive to pollutants and different kinds of stresses and; 5) they provide a suitable model organism for both ecological/developmental studies and biomimetic processes (Pesando et al., 2003; Agnello and Roccheri, 2010; Kobayashi, 1991; Jasny and Prunell, 2006; Wilt, 2005). Sea urchins also offer a cost-effective experimental tool for toxicological studies in biological systems.

There have been several reports published on the use of sea urchins as a biological model to study the influence of toxic materials in the environment. Most of these concern biomimetic processes, focusing on calcification, which is prominent in the construction of skeletons (Bonucci, 2009). The development of sea urchin embryos after fertilization was found to be affected by different types of toxic factors, such as heavy metals (Kobayashi and Ogura, 2004), pesticides (Pesando et al., 2003) and acidic seawater (Moulin et al., 2011) as well as UV-B (Bonaventura et al., 2006) and different gravitational conditions (Marthy et al., 1996), all of which cause abnormal skeletal shapes. Qiao et al. (2003) also demonstrated that sea urchins could serve as a model for mammalian developmental neurotoxicity.

In this work, the *Paracentrotus lividus* sea urchin is chosen as the biological model system, and we present the first reported study of AgNPs therein. We used synchrotron radiation as X-ray source in the measurement, for a number of reasons: it provides much higher intensity than conventional X-ray tubes (resulting in reduced measurement time) and it offers tuneability of the X-ray energy with high collimation (Ide-Ektessabi, 2007), useful for X-ray absorption near edge structure (XANES) spectroscopy to be undertaken in micro-analytical mode. XANES was used to prove the presence and distribution of agglomerated AgNPs which were detected via X-ray fluorescence. When the incident X-ray has an energy equal to that of the binding energy of a core-level electron, there is a sharp rise in absorption. By varying the X-ray energy, the peak of absorbance obviously rises at a particular energy, referred as absorption edge. The exact position of an X-ray core-level absorption edge depends on the chemical environment of an element such as oxidation state, site symmetry, ligands and the nature of bonding (West, 1999). Therefore, XANES is a useful technique for discriminating between Ag present within AgNPs, and its presence in other chemical bonding environments within the sea urchin larva. To complement the XANES work, infrared light from the synchrotron was also used for Fourier transform infrared (FTIR) micro-spectroscopy, which can detect the vibrational bands of functional groups of compounds (Robinson et al., 2005). With the FTIR measurements made in raster-scan mode, several compounds within sea urchin larva can be mapped and characterized in

order to compare the chemical change in the skeleton between AgNP-exposed and control samples.

## 2. Experimental Section

### 2.1. Preparation of Silver Nanoparticles

The silver nanoparticles used in this study were prepared by chemical reduction of silver compounds, following a method used by Link et al. (1999) with a minor modification. 0.0043 g silver nitrate ( $\text{AgNO}_3$ , from Sigma-Aldrich, ACS reagent) was dissolved in 95 mL de-ionised water (Millipore, 18  $\Omega\text{-cm}$ ). The resulting solution was heated by a hot plate to boiling point whereupon 5 mL of sodium citrate (1% w/v, from BDH Chemicals) was added. The solution was then refluxed for 30 minutes and turned into the AgNP suspension. After the suspension temperature decreased to room temperature, it was stored in the dark at 4-8 °C before use. AgNPs produced by this method were found to have a lateral size in the range of 5-35 nm, determined from the images from a high resolution transmission electron microscope (HRTEM) (JEOL 2100F FGETEM) at Durham University.

### 2.2. Preparation of Sea Urchin Specimens

Sperm and eggs (Gametes) were collected from adult sea urchins (*Paracentrotus lividus*) inhabiting the Adriatic Sea at Limski kanal, Croatia. Fertilization, using 0.5 M KCl injection to induce spawning of gametes, was carried out in natural seawater filtered through a 0.22  $\mu\text{m}$  membrane filter. For AgNP-exposed samples (in contrast to the control), about 2 h after fertilization, AgNPs were added to the sea urchin larvae at a concentration of 0.3 mg/L. In both cases, the larvae were collected at 51 h after fertilization by fixing with 100% ethanol. The samples were washed with DI water several times before any measurements.

### 2.3. XANES and FTIR

XANES and FTIR measurements were performed at beamline ID21 of the European Synchrotron Radiation Facility (ESRF), Grenoble, France. XANES spectra were collected in fluorescence mode on selected points of the sample with the beam size of 0.2  $\mu\text{m} \times 0.8 \mu\text{m}$ . Measurements were made using X-rays with tuneable energy in the range from 3.32 to 3.47 keV, with a 0.225 eV energy step and 0.1 s dwell time.

FTIR spectra were collected in transmission mode, with a resolution of 4  $\text{cm}^{-1}$ . The beam size was 6  $\mu\text{m} \times 6 \mu\text{m}$ , imprinting on specimens deposited on 0.2 mm thickness  $\text{BaF}_2$  windows. Specimens were scanned with steps of 4  $\mu\text{m}$  in both directions. For each spectrum, 64 scans were accumulated from 4000 to 500  $\text{cm}^{-1}$  and averaged. Background spectra were collected every 30 minutes.

## 3. Results and Discussion

A typical XANES spectrum is shown in fig. 1a. The spectrum was acquired over the black spot encircled in the

image in fig. 1b (which is an X-ray fluorescence map of the sea urchin larva, recorded at 3.56 keV). The XANES spectra show that the black spots are associated with the presence of agglomerated AgNPs in the sea urchin larvae. The presence of a peak at 3.359 keV in the XANES spectrum, assigned to the  $2p$  to  $5s$  transition of silver (Miyamoto et al., 2010) indicates that the black features are agglomerated AgNPs.

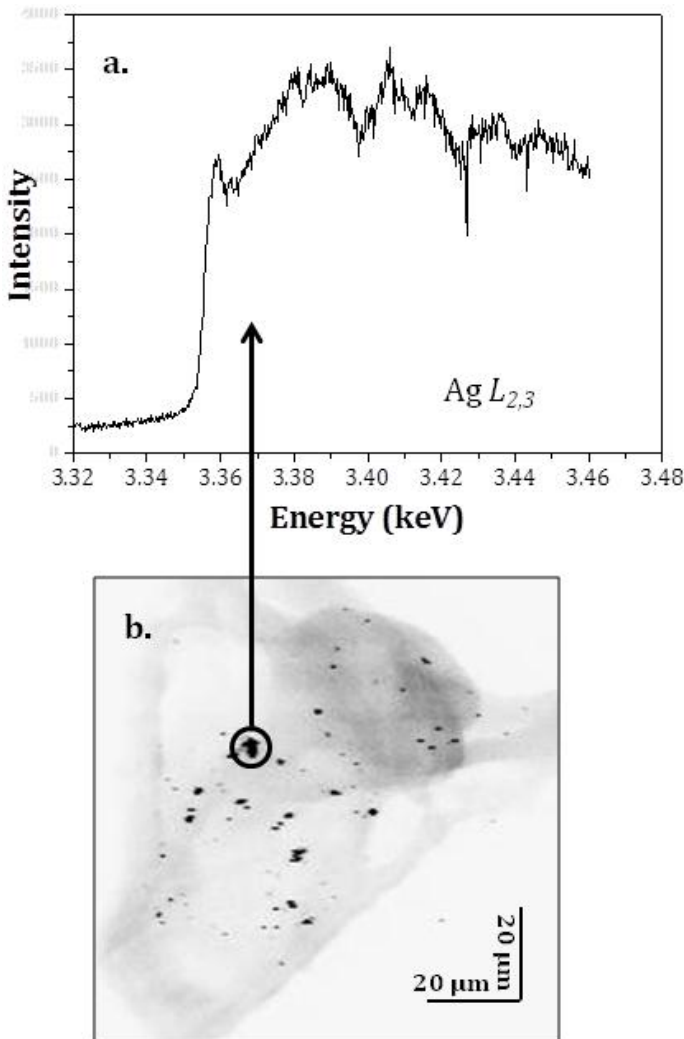


Fig. 1. (a) XANES spectra of the Ag  $L_{2,3}$  edge in the region of the sea urchin embryo indicated by the black circle in (b), using a beam spot size of  $0.2 \mu\text{m} \times 0.8 \mu\text{m}$ , with the pixel size  $0.5 \mu\text{m} \times 0.5 \mu\text{m}$ . (b) the XRF map in reversed grayscale of a sea urchin exposed to AgNPs at concentration of  $0.3 \text{ mg/L}$  after  $51 \text{ h}$  of growth. The size of sea urchin larva image is  $100 \mu\text{m} \times 100 \mu\text{m}$ . The encircled black spot (around  $2-5 \mu\text{m}$ ) indicates the presence of agglomerated AgNPs in sea urchin.

In fig. 2 the XANES spectrum from agglomerated AgNPs in the sea urchins (bottom) is compared with reference spectra from AgCl, Ag foil,  $\text{AgNO}_3$ ,  $\text{Ag}_2\text{O}$ , AgO and  $\text{Ag}_2\text{S}$  (Yin et al., 2011). The data show that the edge of the spectrum from AgNPs in the sea urchins is clearly associated with Ag, but

does not correspond to the reference spectra. Although there is some resemblance of the AgNPs spectrum with that from silver foil, the energy offset of Ag  $L_{2,3}$  edge of nanoparticles and the Ag foil is not the same. There is also a more pronounced peak denoted by dot-dash line (see fig 2) which is not present for Ag foil, so there is additional chemical bonding to the silver present in the AgNPs within the sea urchin. Thus, the agglomerated AgNPs are unlikely to be composed of a single stoichiometric compound.

Comparing the XANES spectrum across the Ag  $L_{2,3}$  edge (fig. 3) from the AgNP exposed sea urchin (red) with the spectrum of AgNPs within *Lolium multiflorum* plants (black) (taken from Yin et al., 2011), it is observed that the lowest energy peak of both spectra is similar. This peak is assigned to oxidized Ag species complexed with S and O/N ligands (Yin et al., 2011). Therefore, the agglomerated AgNPs in sea urchins are likely to contain similar compounds of silver, as observed by Yin et al. (2011).

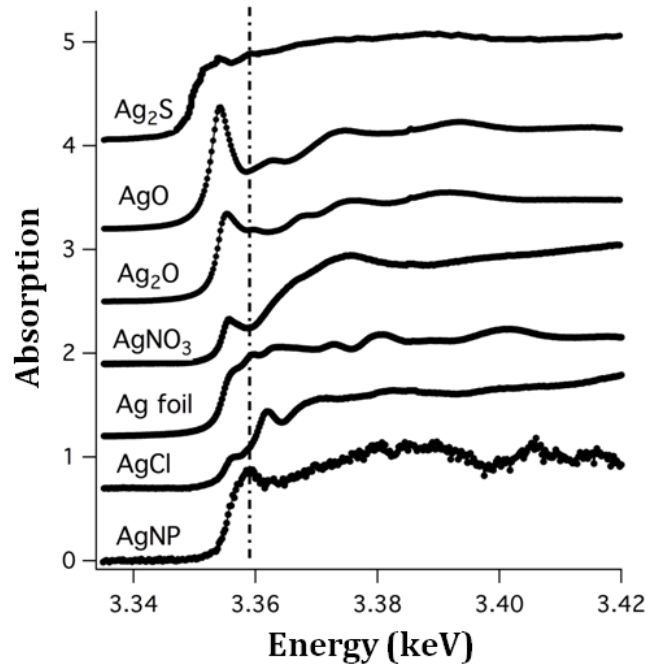


Fig. 2. XANES spectra across the Ag  $L_{2,3}$  edge from a sea urchin exposed to AgNPs at a concentration of  $0.3 \text{ mg/L}$  after  $51 \text{ h}$  of growth (bottom), compared with spectra of AgCl, Ag foil,  $\text{AgNO}_3$ ,  $\text{Ag}_2\text{O}$ , AgO and  $\text{Ag}_2\text{S}$  (The  $\text{Ag}_2\text{S}$  spectrum was taken from Yin et al. (2011)).

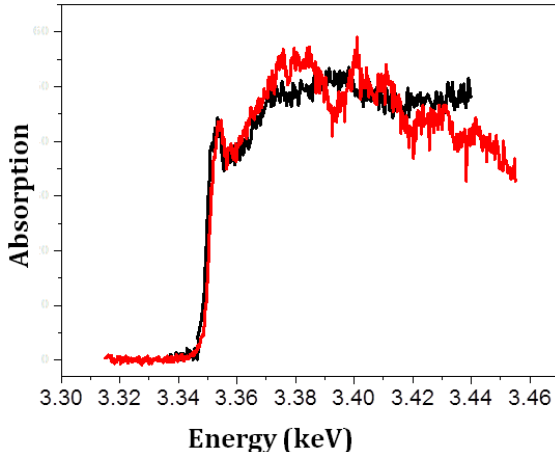


Fig. 3. XANES spectra across the Ag L<sub>2,3</sub> edge from a sea urchin exposed to AgNPs at a concentration of 0.3 mg/L after 51 h of growth (red), compared with the spectrum of AgNPs taken from *Lolium multiflorum* plants (black) from Yin et al. (2011).

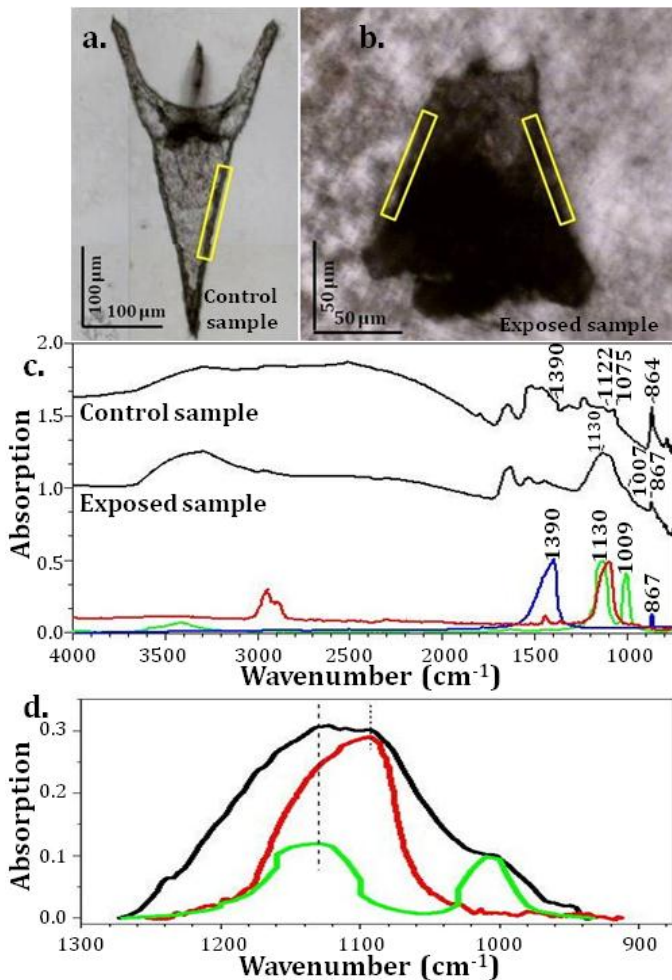


Fig. 4. (a) Control sample at 51 h of growth. (b) A sample exposed to 0.3 mg/L AgNPs after 51 h of growth. (c) FTIR spectra from the control sample (top) and AgNP-exposed sample (bottom) over the regions within the yellow rectangles in (a) and (b), including the reference spectra of calcite (blue), sodium sulphate (red) and sodium thiosulphate (green). (d) The FTIR spectra in the range from 900 to 1300 cm<sup>-1</sup> are enlarged to enable comparison with the spectra of the AgNP exposed sample (black), sodium sulphate (red) and sodium thiosulphate (green). In (c) and (d), FTIR measurement was operated in transmission mode.

sodium thiosulphate (green). (d) The FTIR spectra in the range from 900 to 1300 cm<sup>-1</sup> are enlarged to enable comparison with the spectra of the AgNP exposed sample (black), sodium sulphate (red) and sodium thiosulphate (green). In (c) and (d), FTIR measurement was operated in transmission mode.

The FTIR spectrum was obtained on the selected regions marked in yellow rectangles, seen in fig. 4a (control sample) and in fig. 4b (exposed sample); for comparison, fig. 4c shows reference spectra of calcite (blue), sodium sulphate (Na<sub>2</sub>SO<sub>4</sub>) (red) and sodium thiosulphate (Na<sub>2</sub>S<sub>2</sub>O<sub>3</sub>. 5H<sub>2</sub>O) (green). In fig. 4c, the peak at 864 cm<sup>-1</sup> assigned to calcite in exposed sample is weaker than in control sample, indicating loss of calcite in the exposed sea urchins. One explanation is that silver might inhibit the activity of the carbonic anhydrase enzyme that is responsible for calcite formation in living organisms (Bianchini et al., 2005). Comparison of the FTIR spectra (fig. 4d) of the exposed sea urchin (black) with sodium sulphate (red) and sodium thiosulphate (green) indicates the presence of sulphur-containing compounds. We suggest that the presence of excess sulphur might be the results of a biological response to reduce the concentration of Ag ions (Liu and Hurt, 2010; Ayata and Yildiran, 2005; Feng and van Deventer, 2010). These results correspond to those from XANES discussed above confirming the oxidized Ag species observed are complexed with both S and O/N ligands in AgNP-exposed sea urchins. Further detailed study of FTIR results will be published elsewhere.

#### 4. Conclusion

On exposure of sea urchins to AgNPs at a concentration of 0.3 mg/L for 51 h, agglomerated AgNPs were observed within them. XANES results show that the agglomerated AgNPs might be oxidized and complexed with S and O/N ligands. FTIR measurements confirm the presence of excess sulphur in nanoparticle exposed sea urchins, which is likely to be due to biological processes. In addition, FTIR results illustrate that there is calcite loss from the skeleton of sea urchins, which can be attributed to the inhibition of calcite formation in the presence of AgNPs.

#### Acknowledgements

We thank the EU COST action TD0903 BioMineralix for funding and support, and ONE North East for nanotechnology funding at Newcastle. We grateful acknowledge Martin Paul for taking care of the sea urchins in seawater aquarium in Stuttgart and Sina Hoos for technical assistance. XRF and FTIR studies were funded by grants from ESRF (Project EC-887). SP would like to thank the Royal Thai Government for a scholarship, and UB would like to thank Dr. Carlson with the support work on Titan ChemieSTEM at Eindhoven. We thank M.R.C. Hunt (Durham University) for a reading of the manuscript.

## References

- Agnello, M., Roccheri, M.C. (2010). Apoptosis: focus on sea urchin development. *Apoptosis* 15, 322-330.
- Asharani, P.V., Wu, Y.L., Gong, Z., Valiyaveettil, S. (2008). Toxicity of silver nanoparticles in zebrafish models. *Nanotechnology* 19, 255102.
- Ayata, S., Yildiran, H. (2005). Optimization of extraction of silver from silver sulphide concentrates by thiosulphate leaching. *Minerals Engineering*, 18, 898-900.
- Bar-Ilan, O., Albrecht, R.M., Fako, V.E., Furgeson, D.Y. (2009). Toxicity Assessments of multisized gold and silver nanoparticles in zebrafish embryos. *Small*, 5, 1897-1910.
- Bianchini, A., Playle, R.C., Wood, C.M., Walsh, P.J. (2005). Mechanism of acute silver toxicity in marine invertebrates. *Aquatic Toxicology*, 72, 67-82.
- Bonaventura, R., Poma, V., Russo, R., Zito, F. (2006). Effects of UV-B radiation on development and hsp70 expression in sea urchin cleavage embryos. *Marine Biology* 149, 79-86.
- Bonucci, E. (2009). Calcification and silicification: a comparative survey of the early stages of biomimetic mineralization. *Journal of Bone and Mineral Metabolism*. 27, 255-264.
- Chae, Y.J., Pham, C.H., Lee, J., Bae, E., Yi, J., Gu, M.B., (2009). Evaluation of the toxic impact of silver nanoparticles on Japanese medaka (*Oryzias latipes*). *Aquatic Toxicology*, 94, 320-327.
- Drake, P.L., Hazelwood, K.J. (2005). Exposure-related health effects of silver and silver compounds: A Review. *The Annals of Occupational Hygiene* 49, 575-585.
- Fabrega, J., Luoma, S.N., Tyler, C.R., Galloway, S., Lead, J.R. (2011). Silver nanoparticles: Behavior and effects in the aquatic environment. *Environment International*, 37, 517-531.
- Farkas, J., Christian, P., Urrea, J.A.G., Roos, N., Hassellöv, M., Tollefson, K.E., Thomas, K.V. (2010). Effects of silver and gold nanoparticles on rainbow trout (*Oncorhynchus mykiss*) hepatocytes. *Aquatic Toxicology*, 96, 44-52.
- Feng, D., van Deventer, J.S.J. (2010). Effect of thiosulphate salts on ammoniacal thiosulphate leaching of gold. *Hydrometallurgy*, 105, 120-126.
- Ide-Ektessabi, A. (2007). Applications of synchrotron radiation: Micro beams in cell micro biology and medicine. Springer-Verlag Berlin Heidelberg.
- Jasny, B.R., Prunell, B.A. (2006). The glorious sea urchin-Introduction. *Science*, 314, 938.
- Kobayashi, N. (1991). Marine pollution bioassay by using sea urchin eggs in the Tanabe Bay, Wakayama Prefecture, Japan, 1970-1987. *Marine Pollution Bulletin*, 23, 709-713.
- Kobayashi, N., Okamura, H. (2004). Effects of heavy metals on sea urchin embryo development. 1. Tracing the cause by the effects. *Chemosphere* 55, 1403-1412.
- Link, S., Wang, Z.L., El-Sayed, M.A. (1999). Alloy formation of gold and silver nanoparticles and the dependence of the plasmon absorption on their composition. *Journal of Physical Chemistry B*, 103, 3529-3533.
- Liu, J., Hurt, R.H. (2010). Ion release kinetics and particle persistence in aqueous nano-silver colloids. *Environmental Science and Technology*, 44, 2169-2175.
- Marthy, H.J., Gasset, G., Tixador, R., Schatt, P., Eche, B., Dessommes, A., Giacomini, T., Tap, G., Gorand, D. (1996). The sea urchin larva, a suitable model for biomimetic mineralization studies in space (IML-2 ESA Biorack experiment '24-F urchin'). *J. Biotech.* 47, 167-177.
- Miyamoto, T., Niimi, H., Kitajima, Y., Naito, T., Asakura, K. (2010). Ag  $L_3$ -edge X-ray absorption near-edge structure of  $4d^{10}$  ( $\text{Ag}^+$ ) compounds: Origin of the edge peak and its chemical relevance. *Journal of Physical Chemistry A*, 114, 4093-4098.
- Moulin, L., Catarino, A.I., Claessens, T., Dubois, P. (2011). Effects of seawater acidification on early development of the intertidal sea urchin *Paracentrotus lividus* (Lamarck 1816). *Marine Pollution Bulletin*, 62, 48-54.
- Pearse, J.S. (2006). Ecological role of purple sea urchins. *Science* 314, 940-941.
- Pesando, D., Huitorel, P., Dolcini, V., Angelini, C., Guidetti, P., Falugi, C. (2003). Biological targets of neurotoxic pesticides analysed by alteration of developmental events in the Mediterranean sea urchin, *Paracentrotus lividus*. *Marine Environmental Research*, 55, 39-57.
- Powers, C.M., Yen, J., Linney, E.A., Seidler, F.J., Slotkin, T.A. (2010). Silver exposure in developing zebrafish (*Danio rerio*): Persistent effects on larval behaviour and survival. *Neurotoxicology and Teratology*, 32, 391-397.
- Qiao, D., Nikitina, L.A., Buznikov, G.A., Lauder, J.M., Seidler, F.J., Slotkin, T.A. (2003). The sea urchin embryo as a model for mammalian developmental neurotoxicity: Ontogeny of the high-affinity choline transporter and its role in cholinergic trophic activity. *Environmental Health Perspectives*, 111, 1730-1735.
- Rai, M., Yadav, A., Gade, A. (2009). Silver nanoparticles as a new generation of antimicrobials. *Biotechnology Advances*, 27, 76-83.
- Ringwood, A.H., McCarthy, M., Bates, T.C., Carroll, C.L. (2010). The effects of silver nanoparticles on oyster embryos. *Marine Environmental Research*, 69, S49-S51.
- Robinson, J.W., Frame, E.M.S., Frame II, G.M. (2005). Undergraduate instrumental analysis. 6<sup>th</sup> edition. Marcel Dekker.
- West, A.R. (1999). Basic solid state chemistry. 2<sup>nd</sup> edition. John Wiley & Sons Ltd.
- Wilt, F.H. (2005). Developmental biology meets materials science: Morphogenesis of biomimeticized structures. *Developmental Biology*, 280, 15-25.
- Yeo, M.K., Kang, M., (2008). Effects of nanometer sized silver materials on biological toxicity during zebrafish embryogenesis. *Bulletin Korean Chemical Society*, 29, 1179-1184.

Yin, L., Cheng Y., Epinasse, B., et al. (2011). More than ions:  
The effects of silver nanoparticles on *Lolium multiflorum*.  
Environmental Science and Technology, 45, 2360-2367.

Zuykov, M., Pelletier, E., Demers, S. (2011). Colloidal  
complexed silver and silver nanoparticles in extrapallial  
fluid of *Mytilus edulis*. Marine Environmental Research,  
71, 17-21.